Hypothetical Uninodal Zeolite Structures: Comparison of $AlPO_4$ and SiO_2 Compositions Using Computer Simulation

Alexandra Simperler,[†] Martin D. Foster,[†] Robert G. Bell,*[,†] and Jacek Klinowski[‡]

Davy-Faraday Research Laboratory, The Royal Institution of Great Britain, 21 Albemarle Street, London W1S 4BS, U.K., and Department of Chemistry, University of Cambridge, Lensfield Road, Cambridge, CB2 1EW, U.K.

Received: July 4, 2003; In Final Form: October 29, 2003

A total of 126 hypothetical zeolite structures have been modeled in the composition $AlPO_4$. The framework topologies are those derived by tiling theory and comprise uninodal structures based on simple or quasi-simple tilings. Atomistic calculations have been used to optimize and evaluate each structure, and compare it to that of the SiO_2 polymorph possessing the same topology. Characteristic properties including relative lattice energies, framework density, coordination sequences, accessible volumes, surface areas, average bond distances and angles, and the degree of distortion of the TO_4 tetrahedra were calculated. The AlPOs are found to be more stable relative to berlinite than the zeolites are relative to quartz. The AlPO and SiO_2 polymorphs show the same relationships between framework density and lattice energies, as well as between framework density and accessible volume, enabling us to predict whether individual hypothetical AlPO/silica polymorphs can be expected to be thermodynamically feasible. We describe eight hypothetical AlPO frameworks, which we believe to be interesting and thermodynamically feasible.

1. Introduction

Microporous aluminosilicates and the analogous aluminum phosphates are very important industrially in technologies such as catalysis, sorption, and ion exchange, and new structures with desirable properties, such as versatility, durability, reusability and selectivity, are thus of much interest. Regardless of composition, the structures of such zeolitic materials are based on periodic three-dimensional, 4-connected nets built of TO_4 units.[1,2] Using a combination of geometric and chemical principles, it is therefore possible to generate potential new framework topologies. Indeed many attempts have been made to enumerate possible structures using a variety of computational algorithms, including various systematic and combinatorial methods, as well as to analyze their structures and evaluate their feasibility.[3−11]

Delgado Friedrichs et al.[12] addressed the problem by applying tiling theory to enumerate systematically uni-, bi-, and trinodal 4-connected nets. The structures thus generated were subsequently treated as silica polymorphs and optimized using lattice energy minimization.[13,14] The large number of theoretical nets was reduced by geometrical and thermodynamic criteria to a smaller subset of chemically feasible structures. Choosing the composition SiO_2 for our initial calculations was logical in terms of zeolite chemistry, and because it offered simplicity and internal consistency. However, aluminum phosphates (AlPOs)[15] based on the same types of 4-connected nets also have important practical applications, which inspired us to consider the feasibility of hypothetical AlPO structures, with the aim of identifying similarities and differences between the two classes of compounds, and to determine their stability. While many known aluminum phosphates have isomorphous silica, or aluminosilicate, counterparts, some AlPO structures, such as VPI-5,[16] which contains channels outlined by 18-membered rings, are unique to that composition. Silica polymorphs and aluminum phosphates differ in the nature of bonding: the former consist of covalently bound SiO_4 units, while the latter can be thought of as being built of discrete Al^{3+} and PO_4^{3-} ions.[17] For this reason, and because they have two different types occupying T sites, it is worth investigating whether a different composition results in different framework topologies being favored.

In this article we present the results of lattice energy optimizations of hypothetical AlPOs and compare them to those of their isostructural silica polymorphs. We focus only on uninodal structures, i.e., those with only one topologically distinct T-site. As a measure of relative stability, lattice energies are calculated with respect to berlinite, as those of the silica zeolites are generally quoted with respect to quartz. For both compositions of zeotype, we have examined the dependence of the relative stability on framework densities[18] and on the number of T-sites in the fourth coordination shell.[4] To be useful as a catalyst or sorbent, a chemically feasible structure should comprise voids or channel systems that are accessible from outside of the crystallite. We have calculated accessible volumes and internal surface areas and examined the stability of the various structures as a function of these quantities. Average r(T−O) bond lengths and r(T···T) distances and T−O−T angles have been calculated, as has the difference between the largest and smallest tetrahedral α(O−T−O) angles, to estimate the distortions within a TO_4 unit.

2. Methods

The three-dimensional nets are initially described[12] simply in terms of the relative positions of their vertices (i.e., T-sites). We followed the procedure of Foster et al.[13,14] to generate model silica polymorphs and, from these, the structurally equivalent uninodal AlPOs. The networks of points were converted into chemical structures with oxygen atoms inserted between each pair of adjacent T-sites (Si atoms). Since the initial Si−O−Si angles were 180°, preoptimization with the DLS (distant least

* Corresponding author. E-mail rob@ri.ac.uk; Fax +44 20 7629 3569.
[†] The Royal Institution of Great Britain.
[‡] University of Cambridge.

10.1021/jp035936j CCC: $27.50
Published on Web 12/24/2003

TABLE 1: Framework Type Codes for Microporous Zeolite-type Materials[a]

silicate only	**AFG**(3), **ASV**(2), BEA(9), BIK(2), BOG(6), BRE(4), CAS(3), CFI(5), CON(7), DAC(4), DDR(7), DOH(4), DON(5), **EAB**(2), **EMT**(4), EPI(3), ESV(6), EUO(10), FER(4), **FRA**(6), **GME**(1), GON(4), **GOO**(5), HEU(5), IFR(4), ISV(5), ITE(4), **JBW**(2), **KFI**(1), **LIO**(4), LOV(3), **LTN**(4), MAZ(2), MEI(4), MEL(7), MEP(3), MFI(12), MFS(8), MON(1), MOR(4), **MSO**(3), MTF(6), MTN(3), MTT(7), MTW(7), MWW(8), NAT(2), NES(7), NON(5), **OFF**(2), OSO(2), **PAU**(8), RSN(5), RTE(3), RTH(4), RUT(5), SFE(7), SFF(8), SGT(4),STF(5), STI(4), STT(16), TER(8), TON(4), **TSC**(2), VET(5), VNI(7), VSV(3), YUG(2)
silicate and phosphate	**ABW**(1), **AET**(5), **AFI**(1), **AFX**(2), **ANA**(1), **AST**(2), **ATS**(3), **BPH**(3), **CAN**(1), **CGS**(4), **CHA**(1), **DFT**(1), **EDI**(2), **ERI**(2), **FAU**(1), **GIS**(1), **LAU**(3), **LEV**(2), **LOS**(2), **LTA**(1), **LTL**(2), **MER**(1), **PHI**(2), **RHO**(1), **SOD**(1), **THO**(3)
phosphate only	**ACO**(1), **AEI**(3), AEL(3), **AEN**(3), **AFN**(4), **AFO**(4), **AFR**(4), **AFS**(3), **AFT**(3), **AFY**(2), **AHT**(2), **APC**(2), **APD**(2), **ATN**(1), **ATO**(1), **ATT**(2), **ATV**(2), **AWO**(3), **AWW**(2), **CGF**(5), **CZP**(3), **DFO**(6), **OSI**(3), **SAO**(4), **SAS**(2), **SAT**(2), **SAV**(3), **SBE**(4), **SBS**(4), **SBT**(4), **VFI**(2), WEI(2), **ZON**(4)

[a] Upper row: silicates only; middle row: both silicates and phosphates; lower row: phosphates only. The numbers in parentheses indicate the number of crystallographically distinct T-sites. Bold print indicates the framework types without odd numbered rings.

squares) method[19] was used to reduce these to more realistic values <180°, thus producing a more accurate starting structure for further calculations. However, when this resulted in unrealistically short Si···Si distances, the angle was left at 180°. Lattice energy minimization with GULP[20] was then performed using the ionic potential model of Sanders et al.[21] Calculations were performed under constant pressure conditions, i.e., cell parameters were allowed to vary as well as atomic and shell coordinates, and no internal symmetry was assumed. Foster et al.[13,14] optimized the structures of 167 uninodal silica polymorphs enumerated using tiling theory, of which 59 were duplicates. Of the remaining 108 structures, 9 had the same topologies as others, but with qualitatively different structures arising from different space group definitions, and 21 known framework types were identified.

The AlPO structures were obtained using an equal number of strictly alternating P and Al atoms at T-sites. Structures containing odd-membered rings were thus excluded, as they did not allow the Al/P ratio of 1:1, as demanded by charge neutrality. A total of 134 uninodal hypothetical silica polymorphs had suitable AlPO counterparts, and the structures were optimized with GULP using the potentials of Gale and Henson.[22] Seven structures could not be optimized due to possessing highly strained geometries. Fifty-two were identical duplicates of others, a further 9 had duplicate framework topologies but qualitatively different structures, and the 21 "real" framework types were identified (though obviously not all of these are known in an AlPO composition). For comparison we also optimized as AlPOs all the existing framework types in zeolite *Atlas*,[23] which have even-membered rings. For most of these, the starting structures were taken from those in the database of the *Cerius2* software package.[24] We treated the known frameworks as silica polymorphs or AlPOs with Al/P = 1:1. Table 1 lists all known AlPO structures and indicates the number of topologically distinct T-sites in parentheses. Structures without odd-membered rings are indicated by bold print. We refer to the hypothetical AlPO and silica polymorphs as hyp-AlPO and hyp-ZEO, respectively, and to the AlPO and silica polymorphs of known framework types as known-AlPO and known-ZEO, respectively. Note that the "known-" prefix indicates simply that the framework type is to be found in the zeolite *Atlas*, not necessarily that it exists in an $AlPO_4$ or high silica form. The energy data and related quantities are those derived from the GULP minimizations, while the average bond distances, angles, and connectivity data were obtained using *zeoTsites* (version 1.2).[25]

To calculate the accessible volume and surface area, we used the Free Volume module of the *Cerius2* package.[24] This applies the Connolly method,[26] consisting of "rolling" a probe sphere with a radius of 1.4 Å over the van der Waals' surface of the framework atoms (using the van der Waals' radii of 1.32, 0.9, 1.05, and 0.85 Å for O, Si, Al, and P, respectively). The void volume was obtained first, and by forcing the probe molecule to enter the unit cell from the outside, the accessible volume was calculated. The Connolly surface is the surface enclosing the void volume.

TABLE 2: Experimental Values of Enthalpies of Transition, $\Delta H_{trans,298K}$, and Calculated Lattice Energies, ΔE_{latt}, of AlPOs and ZEOs per TO_2 unit

	$\Delta H_{trans,298K}$ $(AlPO)_{exp}$ [kJ/mol]	$\Delta H_{trans,298K}$ $(ZEO)_{exp}$ [kJ/mol]	$\Delta E_{latt,berlinite}$ [kJ/mol]	$\Delta E_{latt,quartz}$ [kJ/mol]
α-cristobalite	3.05[a]	2.48[b]	−1.50	3.22
AEL	6.19[a]		4.03	10.99
AET	5.77[a]		7.32	14.44
AFI	7.01[a]	7.20[c]	5.35	11.68
AST		10.86[d]	11.38	18.14
BEA		9.29[d]		14.39
CFI		8.82[d]		13.00
CHA		11.43[d]	8.65	16.30
FAU		13.60[c]	13.20	19.91
FER		6.60[c]		11.78
IFR		10.04[d]		15.00
ISV		14.37[d]		16.44
ITE		10.08[d]		14.12
LTA	7.78[a]		11.66	19.26
MEI		13.90[e]		
MEL		8.19[d]		10.76
MFI		6.78[d]		9.96
MTW		8.70[c]		8.14
MWW		10.42[d]		14.68
STT		9.19[d]		14.70
VFI	8.37[a]		10.95	21.12

[a] Reference 27. [b] Reference 28. [c] Reference 29. [d] Reference 18. [e] Reference 30.

3. Results and Discussion

Energy. Table 2 lists the experimentally obtained enthalpies[18,27−30] for a selection of known-AlPO and known-ZEO structures and their calculated relative lattice energies. Figures 1a,b show the plots of the calculated relative lattice energies of AlPO and ZEO, $\Delta E_{latt,berlinite} = E_{latt,AlPO} - E_{latt,berlinite}$, and $\Delta E_{latt,quartz} = E_{latt,ZEO} - E_{latt,quartz}$, vs the experimental enthalpy, $\Delta H_{trans,298K}$, of the transitions from berlinite to AlPO and α-quartz to SiO_2 polymorph at 298 K. The AlPO data were calculated via a thermodynamic cycle by Hu et al.,[27] who found that microporous AlPO frameworks are energetically less stable than berlinite by only 11−17 kJ/mol. Because of the limited availability of experimental AlPO results, we could not deduce a strong correlation between experimental and theoretical data, but the calculated lattice energies reproduce the trend of the experimental data (Figure 1a). The calculated values are in agreement with the results of Henson et al.,[31] who claim that the agreement between their calculations and experimental data for AlPOs is

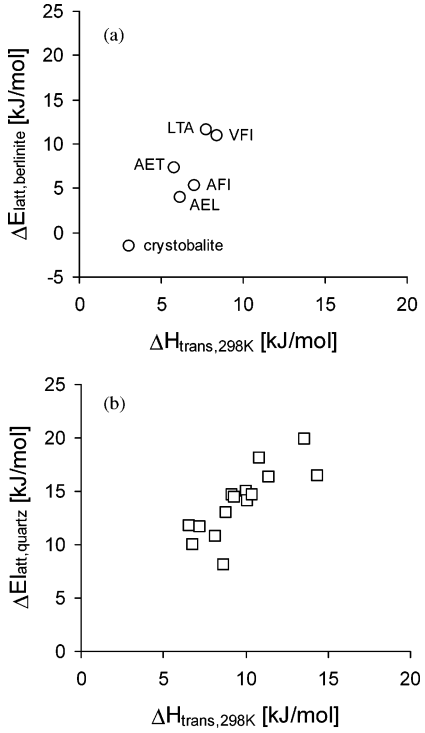

Figure 1. Calculated relative lattice energy (a) $\Delta E_{\text{latt,berlinite}}$ and (b) $\Delta E_{\text{latt,quartz}}$ vs the corresponding experimental enthalpy, $\Delta H_{\text{trans,298K}}$.

not as good as those for silica polymorphs. While the ionic potential model used cannot fully represent the subtleties of bonding in these materials, it predicts that more dense structures would be more thermodynamically stable. Petrovic et al.[29] and Piccione et al.[18] found the enthalpies of a range of silica polymorphs to be 7−14 kJ/mol less stable than quartz. Figure 1b reveals a very good correlation between experimental and calculated data, similar to that found by Henson et al.[32]

Figures 2a−c show the calculated lattice energies of the known-AlPO and hyp-AlPO ($\Delta E_{\text{latt,berlinite}}$, relative to berlinite) in order of increasing energies and their isostructural known-ZEOs and hyp-ZEOs ($\Delta E_{\text{latt,quartz}}$, relative to quartz). Both known-AlPO and known-ZEO in Figure 2a show the same stability trend, though the known-AlPOs are more stable relative to berlinite than their isostructural silica polymorph is relative to quartz. If defect-free, the known structures can be up to 50 kJ/mol less stable than berlinite/quartz. Figure 2b gives the plot for the hypothetical structures, showing that hypothetical structures can be as much as 500 kJ/mol less stable than the reference structures. As structures more than 100 kJ/mol less stable than berlinite or quartz are unlikely to be feasible, Figure 2c shows only the 0−100 kJ/mol region. The hyp-AlPO isostructural form with the less stable hyp-ZEOs ($\Delta E_{\text{latt}} > 80$ kJ/mol) is predicted to be more stable with respect to berlinite than their silica counterparts are with respect to quartz. The reason is that the Gale and Henson potentials overestimate the strength of the Al−O bond, and thus add attractive interactions to the total lattice energy. We will concentrate on structures with $\Delta E_{\text{latt}} < 80$ kJ/mol, where the potentials give a more accurate representation of the Al−O bond strength.

Framework Density and the Coordination Sequence. Figures 3a,b show plots of the relative lattice energy versus framework density, FD,[33] which is defined as the number of T-sites per 1000 Å^3 for the known and hypothetical structures. For the sake of completeness, Figure 3b contains structures up to 100 kJ/mol less stable than berlinite/quartz. The known-AlPO and known-ZEO show a linear correlation between the two

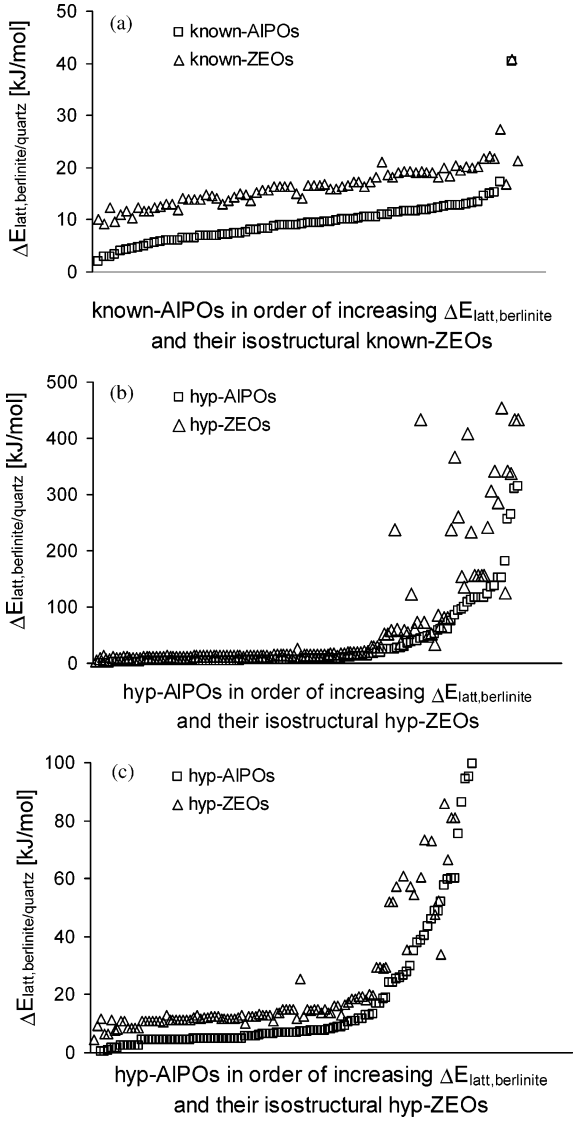

Figure 2. Calculated relative lattice energies of (a) the known-AlPOs in order of increasing energies and their isostructural known-ZEOs; (b) of the hyp-AlPOs in order of increasing energies and their isostructural hyp-ZEOs; and (c) of the hyp-AlPOs in order of increasing energies and their isostructural hyp-ZEOs with ΔE_{latt} in the 0−100 kJ/mol range.

quantities, with frameworks of high density being more stable than those with lower FD (Figure 3a). The latter are thermodynamically less stable due to increased void volumes, which generally come at an energetic cost.[18] This correlation is the decisive criterion as to whether a hypothetical structure is thermodynamically feasible. The FDs are between 13 and 20 T-sites per 1000 Å^3 for the known frameworks, and 26.2 for berlinite and 27.7 for quartz, respectively. The known framework of CZP is observably less stable than the majority of other frameworks, either as AlPO or ZEO. Figure 3b shows the same plot for the hypothetical structures, including structures with ΔE_{latt} up to 100 kJ/mol. In addition to a concentration of structures in the low energy/low-density region occupied by the known topologies, a number of less feasible structures are observed, including several of higher density than quartz or berlinite. It also shows that all structures are above an FD of 10 T-sites per 1000 Å^3, in agreement with Hyde et al.,[34] who claim a minimum value of 10.7 T-sites per 1000 Å^3 due to geometric considerations. For the hypothetical structures we obtained FDs of up to 47 per 1000 Å^3, although many of these were of extremely high

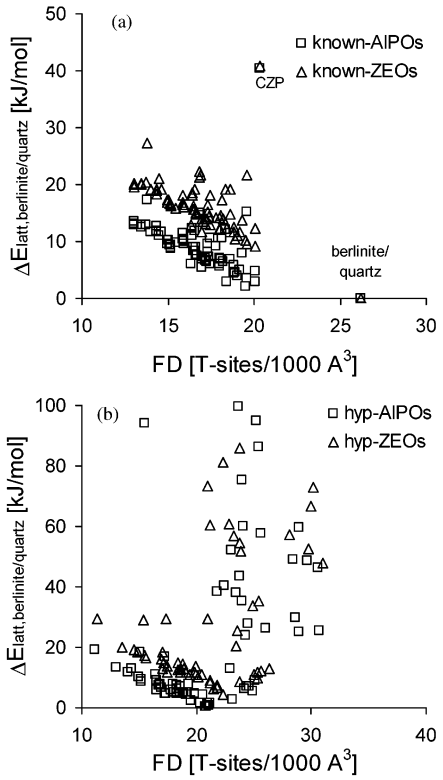

Figure 3. Relative lattice energy, $\Delta E_{\text{latt,berlinite/quartz}}$, vs. framework density, FD, for (a) known and (b) hypothetical structures.

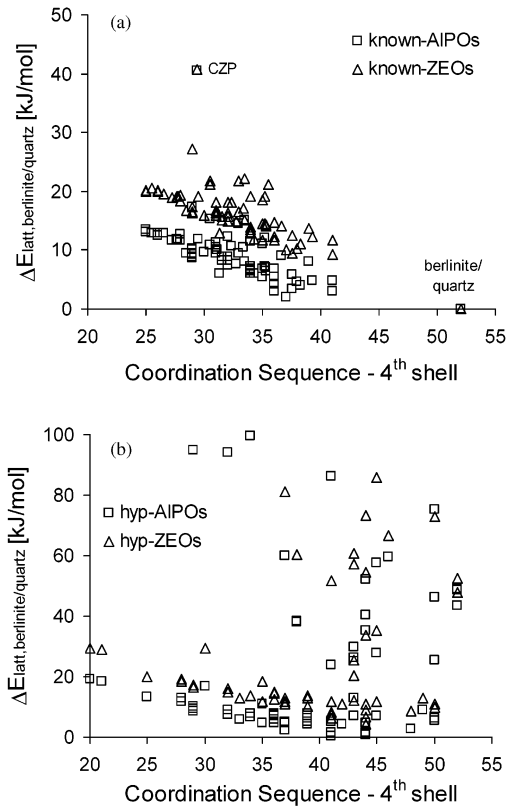

Figure 4. Relative lattice energy, $\Delta E_{\text{latt,berlinite/quartz}}$, vs. coordination sequence of the fourth shell for (a) known and (b) hypothetical structures.

ΔE_{latt} (not shown in Figure 3b) and could not be optimized effectively in either $AlPO_4$ or SiO_2 form. Hence, we can define a region of lattice energy and FD in which a structure has to fall in order to be feasible. Hypothetical structures up to 20 kJ/mol less stable than their reference frameworks (berlinite or quartz) clearly fulfill these conditions and, in general, most of the less stable structures have appreciably higher densities. Although we have seen that higher density generally results in greater stability within the "zeolitic" range of density, in cases where the density is equivalent to, or greater than, dense mineral phases, structures are often much less stable due to increased repulsion and distortion of the tetrahedral units.

Figures 4a,b show plots of relative lattice energies vs the number of T atoms in the fourth coordination shell. These plots resemble the plots in Figures 3a,b as the population of the fourth shell can also be seen as a measure of the density of the framework.[4] Each T atom is connected to four neighbors in the first shell, and these four T atoms themselves can have up to 12 neighbors in the second shell, and so on. Generally, the *maximum* population of the *k*th shell is[23] $N_k \leq 4 \times 3^{k-1}$; so the fourth shell can contain no more than 108 T atoms. As every T atom is counted only once, lower numbers indicate the presence of rings within a framework, usually outlining channel walls or openings of voids. Hence, a low coordination sequence (CS) number is associated with a less dense structure, with channels and voids, and the structure is therefore thermodynamically less stable. This trend is evident in Figure 4a, which shows data for the known framework types. As we also included polynodal structures in this graph, the CS was obtained by taking the average value for the CS of the crystallographically different T-sites. For the known frameworks (structures with odd numbered rings excluded) we find fourth CS values between 25 and 41, while the fourth CS for berlinite/quartz is 52. The hypothetical structures have CS in the fourth shell of 20−52. Figure 4b shows that hypothetical structures with higher CS values are less stable due to high density. A region of linear dependence between the fourth CS and relative lattice energy can be clearly recognized, and structures with data in this linear region can be considered as chemically feasible.

Accessible Volume and Surface Area. Besides identifying feasible structures by the stability criteria considered above, we want to predict and describe structures of practical interest, in the first instance microporous frameworks containing channels and/or voids. The amount of void volume as well as its accessibility (whether a molecule can enter the structure from the outside) is thus of interest. We have examined the trends of the accessible volume with respect to the framework density and the relative stability for known and hypothetical structures. As described previously, the void volume is calculated with respect to a probe of 1.4 Å radius. The accessible volume for known-AlPO and known-ZEO is in the range of 0−28 Å^2 per T-site. As compact materials, quartz and berlinite have zero accessible volume.

Figure 5a shows a strong linear correlation between accessible volume and FD. The structures of AST and MSO, with apertures formed exclusively by 6-rings, are too narrow to admit the probe molecule[26] and have zero accessible volume either as an AlPO or as a ZEO structure. Figure 5b shows the trends of accessible volume with increasing lattice energy for existing structures. With higher values of the accessible volume and larger void and channel openings, the structure becomes less thermodynamically stable. Hyp-AlPO and hyp-ZEO can have volumes up to 45 Å^2 per T-site and structures with FD above 20 show hardly any accessible volume. The plot of accessible volume vs relative lattice energies in Figure 5d shows that structures which are less stable by 20 kJ/mol than berlinite/quartz have very little accessible volume. This is in accordance with the

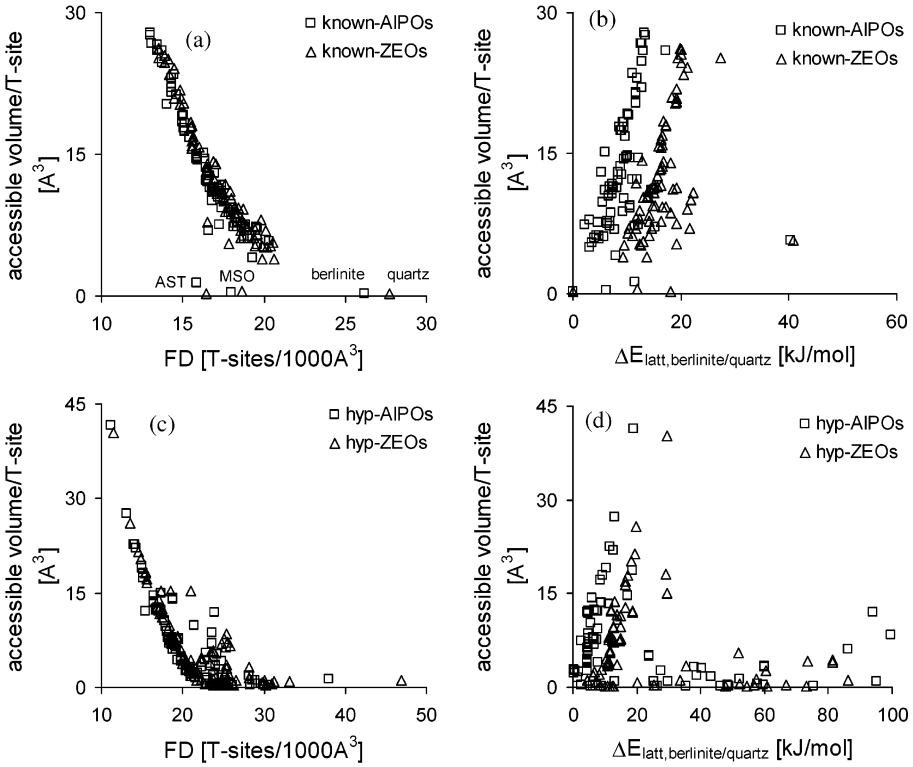

Figure 5. Accessible volume per T-site vs framework density, FD, for (a) known and (c) hypothetical structures. Accessible volume per T-site vs relative lattice energy, $\Delta E_{\text{latt,berlinite/quartz}}$, for (b) known and (d) hypothetical structures.

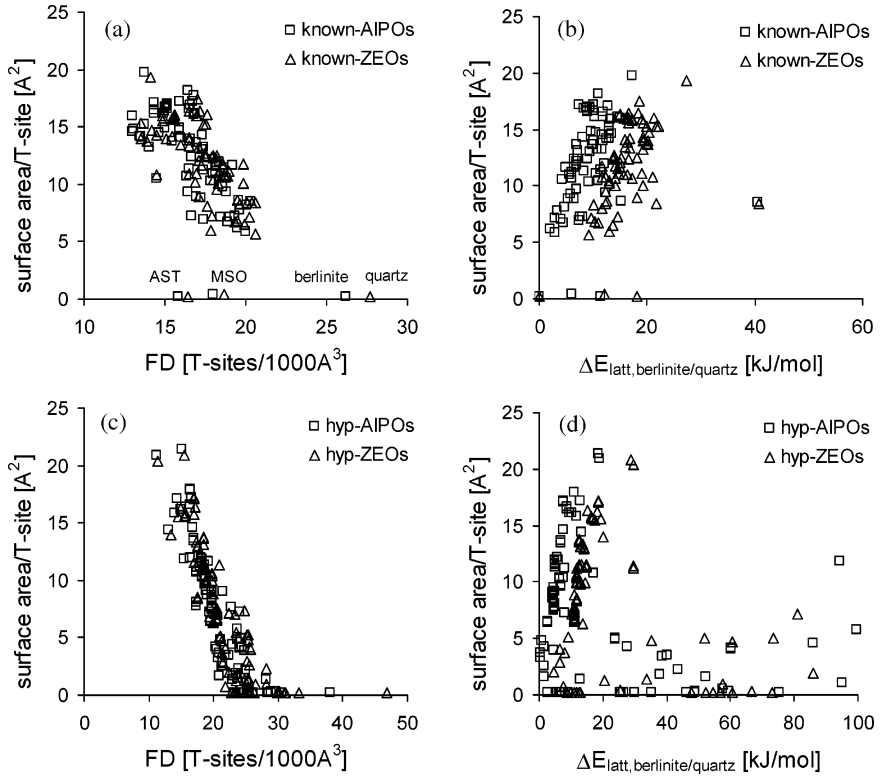

Figure 6. Surface area per T-site vs framework density, FD, for (a) known and (c) hypothetical structures. Surface area per T-site vs relative lattice energy, $\Delta E_{\text{latt,berlinite/quartz}}$, for (b) known and (d) hypothetical structures.

observation that very dense structures (those with small accessible volumes) are less stable.

Another important characteristic of a good catalyst or sorbent is the amount of internal surface area[35] on which reaction or sorption takes place. Figures 6a−d show plots of the surface area per T-site vs FD and ΔE_{latt} for the known and hypothetical structures. Since the surface is defined as the envelope of the accessible volume, the same trends can be found. AST, MSO, berlinite, and quartz have no surface area since they have no accessible volume (Figure 6a). The surface areas of the known frameworks are 5−20 Å^2 per T-site per unit cell. For existing frameworks, we find that increasing surface area is in general

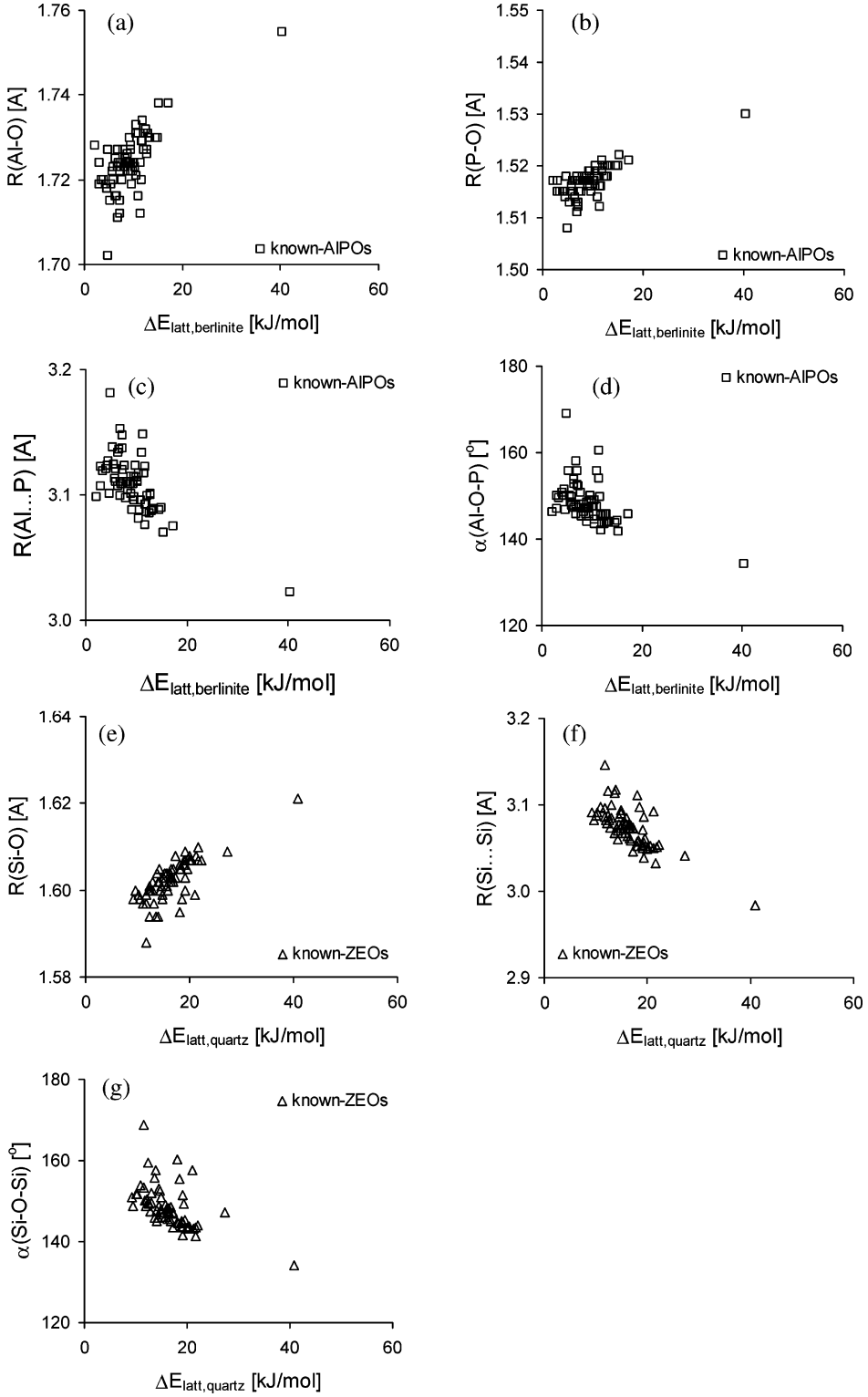

Figure 7. Average bond lengths (a) r(Al−O), (b) r(P−O), and (e) r(Si−O); bond distances (c) r(Al···P) and (f) r(Si···Si), and bond angles (d) α(Al−O−P) and (g) α(Si−O−Si) vs relative lattice energy, $\Delta E_{\text{latt,berlinite/quartz}}$, for known-AlPOs and known-ZEOs.

accompanied by decreasing stability (Figure 6b), although there is considerable scatter in the data. The uninodal hypothetical frameworks show at maximum a surface area of 21 Å^2/T-site, and a higher FD is accompanied by reduced surface area (Figure 6c). Figure 6d shows that the approximately linear relationship between surface area and relative lattice energy holds for $\Delta E_{\text{latt}} < 20$ kJ/mol. Above this value, the structures are too dense to be stable.

Geometry. Figures 7 and 8 show the results of the average bond distances, r(T−O) and r(T···T), and average α(T−O−T) angles for known and hypothetical structures. Figures 7a−d give the average geometry data of the known-AlPO, which have r(Al−O) bond lengths in the 1.70−1.76 Å range and average r(P−O) bond lengths in the 1.51−1.54 Å range. The ranges covered are just 0.05 Å for R(Al−O) and 0.03 Å for R(P−O). When the values for the CZP structure type (the data point of 43.83 kJ/mol, furthest to the right in Figures 7a−d) is excluded, the ranges are below 0.02 Å. The distances between the adjacent T-sites, r(Al···P), are found to be above 3.0 and 3.2 Å and are also distributed over a small range. The angle, α(Al−O−P),

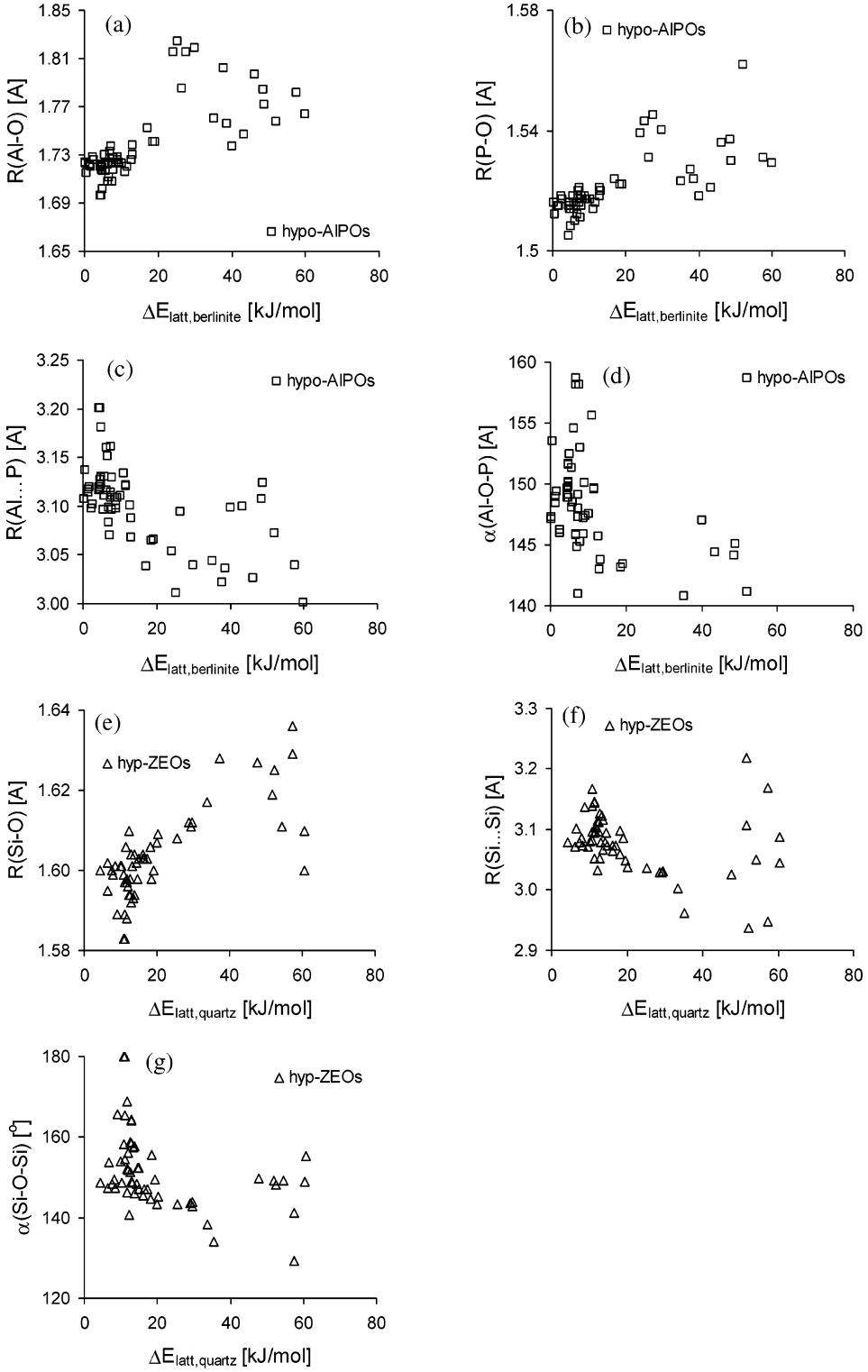

Figure 8. Average bond lengths (a) r(Al−O), (b) r(P−O), and (e) r(Si−O); bond distances (c) r(Al···P), (f) r(Si···Si), and bond angles (d) α(Al−O−P) and (g) α(Si−O−Si) vs relative lattice energy, $\Delta E_{\text{latt,berlinite/quartz}}$, for hyp-AlPOs and hyp-ZEOs.

covers a range from 134 to 169°, including the less stable CZP. Excluding it will leave us with an angle of 140° as the "minimum value" for reasonable geometry. The known-ZEO geometry data are graphically shown in Figures 7e−g, and the plot in Figure 7e shows the 1.58−1.62 Å range for the average bond distances r(Si−O), also covering a small range.

The distance between two next-neighbor T atoms, r(Si···Si), is closely distributed around 3.08 Å, and the angles α(Si−O−Si) are 140−160°, comparable with the known-AlPO. There is no apparent linear relationship between stability and geometry data, and the bond lengths in particular do not vary much between the different structures. Hence, geometry data of a hypothetical structure considered as being feasible should lie within the suggested ranges. Figures 8a−g show similar plots for the hyp-AlPO and hyp-ZEO. We discuss only hypothetical structures up to 60 kJ/mol less stable than berlinite or quartz, as above that value the connectivity of the structures is not clearly identified. Structures with high FD no longer show a clear distinction between TO_4 units, so an evaluation of connectivity becomes more unreliable. Nevertheless, the dataset

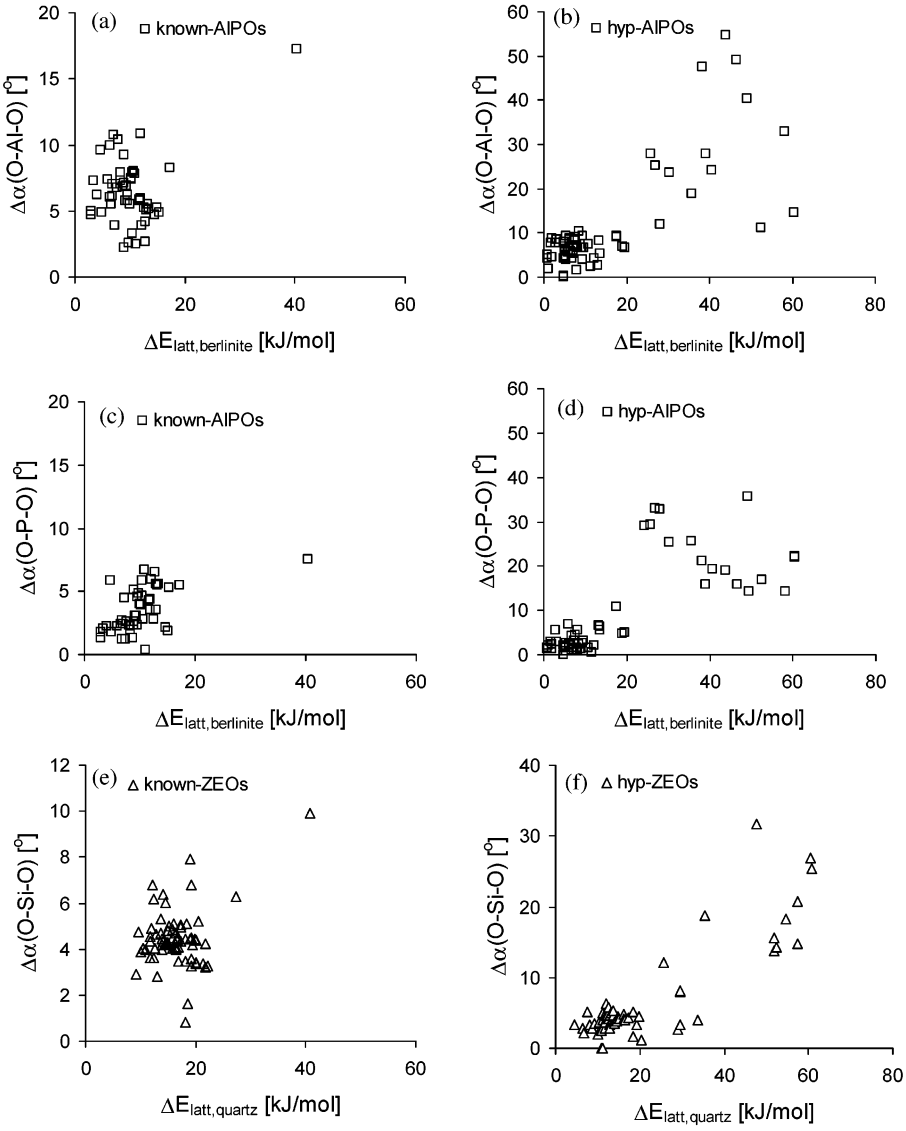

Figure 9. Difference between the largest and smallest α(O−Al−O) tetrahedral angle, Δα(O−Al−O), vs relative lattice energy, $\Delta E_{\text{latt,berlinite}}$, for (a) known-AlPOs and (b) hyp-AlPOs; difference between the largest and smallest α(O−P−O) tetrahedral angle, Δα(O−P−O), vs relative lattice energy, $\Delta E_{\text{latt,berlinite}}$, for (c) known-AlPOs and (d) hyp-AlPOs; and difference between the largest and smallest α(O−Si−O) tetrahedral angle, Δα(O−Si−O), vs relative lattice energy, $\Delta E_{\text{latt,quartz}}$, for (e) known-ZEOs and (f) hyp-ZEOs.

is representative enough to give a clear picture. In Figures 8a,b the average distances *r*(Al−O) and *r*(P−O) show two clear distributions of data points, below and above 20 kJ/mol relative stability. Below, most data points are found between 1.7 and 1.75 Å, in a similar range to the data of the known frameworks. Above 20 kJ/mol, the average bond lengths are longer: up to 1.82 Å. For the hypothetical structures, the average distances between two adjacent T-sites, *r*(Al...P) in Figure 8c, are smaller (below 3.1 Å) in less stable frameworks. In Figure 8d, the angles α(Al−O−P) are all in the 140−160° range, although some less stable structures have smaller angles. Figures 8e−g show the data for the isostructural hyp-ZEO, which are again similar to the hyp-AlPO data. The *r*(Si−O) bond lengths are longer within less stable silica polymorphs (up to 1.64 Å), while the *r*(Si⋯Si) distances are not very different from those in the more stable frameworks. A few α(Si−O−Si) angles in less stable structures are found to be below 140° for structures with $\Delta E_{\text{latt}} > 20$ kJ/mol, and some of the more stable structures have values up to 180°, thus covering a larger range than their isostructural hyp-AlPO form.

To examine the magnitude of distortion of TO_4 units, we calculated the difference between the largest and smallest tetrahedral angles, Δα(O−T−O) (Figures 9a−f). The average difference is indicative of the strain in the zeolitic TO_4 units, since a distorted TO_4 unit is less stable. Figures 9a and 9c show plots of Δα(O−Al−O) and Δα(O−P−O), respectively, vs ΔE_{latt} for the known-AlPO. Again, we exclude the values for CZP (the data point furthest right in Figures 9a and c) and find differences between the tetrahedral angles in AlO_4 units between 2 and 11° (Figure 9a) and in PO_4 units between 0 and 7° (Figure 9c). For SiO_4 units in known-ZEO, the average Δα(O−Si−O) values range between 0 and 7°, similar to PO_4 units in known-AlPO. These differences can partly be explained by the larger size of aluminum, as well as considerations of ionicity[17] within the AlPO framework which allows a greater distortion of the TO_4 units. Figures 9b, d, and f the show the corresponding data for the hypothetical frameworks. The Δα(O−T−O) values of all the structures with $\Delta E_{\text{latt}} < 20$ kJ/mol are found in the same regions as for the corresponding known structures. Hypothetical structures with $\Delta E_{\text{latt}} > 20$ kJ/mol have distorted TO_4 units: Δα(O−P−O) is in the 7−30° range, and Δα(O−Si−O) is in

TABLE 3: Ranges of Characteristic Physical Properties of All Known-AlPOs and Known-ZEOs, and Hypo-AlPOs and Hypo-ZEOs with $\Delta E_{latt} < 20$ kJ/mol

	known-AlPOs	known-ZEOs	hypo-AlPOs	hypo-ZEOs
FD[T-sites/1000 Å^3]	13.02−20.33	12.80−21.05	11.12−25.15	13.50−26.33
coordination sequence−fourth shell	25−41	25−41	20−50	20−50
accessible volume/T-site [A^3]	0.00−25.59	0.00−27.07	0.00−41.27	0.00−25.63
surface area/T-site [A^2]	0.00−19.58	0.00−23.28	0.00−21.20	0.00−17.04
R(T−O) [Å][a]	1.70−1.76 1.51−1.54	1.59−1.63	1.70−1.75 1.51−1.52	1.58−1.61
R(T···T) [Å]	3.02−3.18	2.94−3.16	3.04−3.20	3.03−3.17
α(T−O−T) [°]	134.23−169.23	129.32−174.38	136.91−180.00	140.80−180.00
α(O−T−O) [°][a]	109.30−109.49 108.66−109.49	109.46−109.49	109.42−109.52 109.33−109.49	109.46−109.49
Δα(O−T−O) [°][a]	2.22−17.29 0.42−11.52	0.81−9.92	0.00−10.41 0.00−10.80	0.00−6.35

[a] For AlPOs: upper value T = Al, lower value T = P.

the 6−32° range, while the AlO_4 units are more distorted with Δα(O−Al−O) in the 10−55° range. O−T−O angle terms constitute only a very small part of the force field energy, and in general the distortion of the TO_4 units seems a good measure of the degree of strain within a structure.

General Comparison with Known Structures. In Table 3 we summarize data for all known framework topologies (i.e., not just uninodal), minimized as SiO_2 polymorphs (ZEO) and as $AlPO_4$, using the same potentials as for the hypothetical structures. The quantities are given in the form of ranges found within that set of structures, and are compared to those of hypothetical AlPO and ZEO structures with $\Delta E_{latt} < 20$ kJ/mol. Comparing known with hypothetical, it can be seen that the ranges covered are closely similar for each composition, i.e., using the ranges defined by the "feasible" hypothetical structures, there are no known frameworks which stand prominently outside this parameter space (with the exception of CZP which, as already mentioned, has ΔE_{latt} greater than 20 kJ/mol). One quantity which occupies a slightly greater range for known than for hypothetical zeolites is Δα(O−T−O), a measure of distortion of the coordination tetrahedra. A further point to note is the large discrepancy in maximum accessible volume between hypo-AlPOs and hypo-ZEOs. This is simply due to the fact that structure 1_11, which has by far the largest accessible volume, falls below $\Delta E_{latt} = 20$ kJ/mol in the AlPO composition, but not in the ZEO.

A Selection of Hypothetical Structures. We have selected eight structures with $\Delta E_{latt} < 20$ kJ/mol, which we considered as chemically feasible and which show features relevant for experimentalists, such as a continuous channel system and/or large voids: (a) AlPO_1_272, (b) AlPO_1_195, (c) AlPO_1_120, (d) AlPO_1_122, (e) AlPO_1_73, (f) AlPO_1_66, (g) AlPO_1_14, and (h) AlPO_1_11, listed in order of decreasing stability (Figure 10a−h). Table 4 lists the most important data for these hypothetical AlPOs as well as their isostructural hypothetical silica polymorphs. Note that the numbering AlPO_1_*n* refers to structures in our database and not to the AlPO-*n* convention used to identify known AlPO structures.

Several hypothetical structures have a high density, such as AlPO_1_272 (Figure 10a), which is a good example. Because of their zero accessible volume, these structures are not promising candidates for catalytic applications. The pore size (defined as in ref 23 with van der Waals radius of oxygen 1.35 Å) of the 6-rings is 2.4 × 2.4 Å for AlPO_272 and 2.5 × 2.5 Å for the corresponding silica polymorph. AlPO_195 (Figure 10b) seems more promising, with its one-dimensional channel system of elongated 8-rings, four of them spirally orientated around connecting 4-rings. The 8-rings have a pore size 1.9 × 6.4 Å and the structure has a small accessible volume of 2.45 Å^3/T-site. The ZEO version is slightly less elongated with a pore size of 2.7 × 5.8 Å and the accessible volume is 4.39 Å^3/T-site, slightly more accessible. AlPO_1_120 (Figure 10c) also has an 8-ring channel system with the pore size of 3.0 × 5.5 Å (2.7 × 5.5 Å for ZEO_1_120) and four 8-ring channels arranged around a connecting 4-ring. The accessible volumes are 5.6 Å^3/T-site for AlPO_120 and 7.11 Å^3/T-site for ZEO_1_120, respectively. AlPO_1_122 (Figure 10d) is similar in stability and density to AlPO_1_120, except that 6- and 4-rings are connecting the 8-ring channels. AlPO_1_73 (Figure 10e) contains large 12-membered rings arranged on a hexagonal lattice with a pore size of 7.1 × 7.4 Å (7.0 × 8.0 Å for ZEO_73), and with an accessible volume of 14.17 Å^3/T-site (13.52 Å^3/T-site for ZEO_1_73). This structure is interesting for catalysis and adsorption. Another structure comprising 12-membered rings is AlPO_1_66 (Figure 10f) with pore sizes similar to AlPO_1_73, but more than 50% less stable. AlPO_14 (Figure 10e) contains elongated 12-membered rings (2.9 × 9.3 Å for both AlPO and ZEO structures) running perpendicular to each other and its accessible volume is 18.46 Å^3/T-site (17.86 Å^3/T-site for the isostructural ZEO). An example for a cage structure is AlPO_1_11 (Figure 10f), where the cages are connected by 8- and 12-membered rings. The pore sizes of the eight-membered rings and of the 12-membered rings are 4.2 × 4.5 Å and 6.1 × 6.6 Å, respectively (3.9 × 4.4 Å and 6.1 × 6.6 Å for the ZEO versions, respectively). Both AlPO_11 and ZEO_11 have an accessible volume of ca. 40 Å^3/T-site.

4. Conclusions

A comparison of known and hypothetical uninodal aluminum phosphates and their isostructural silica polymorphs reveals more similarities than differences between the two groups of structures. Calculations of relative stabilities showed the AlPO to be more stable relative to berlinite than the silica polymorphs are with respect to quartz. With only a very few exceptions, the stability sequences of AlPO and ZEO frameworks show similar trends for the 80 most stable structures. With more dense structures, the potential model fails to represent the strength of the Al−O bonds, overestimating the stability of the AlPO. A correlation between the relative lattice energies and framework densities has a linear region ($\Delta E_{latt} = 0-20$ kJ/mol) for both classes of compounds. Within this region, structures with low framework density are less stable. Structures with too high density are thus less stable, as increased density leads to a higher compression of atoms, which is unfavorable. For both the AlPO and ZEO we find similar trends in the dependence of stability on the framework density, so that hypothetical structures in this linear region can be considered as feasible. We obtained the same result when considering correlations between relative

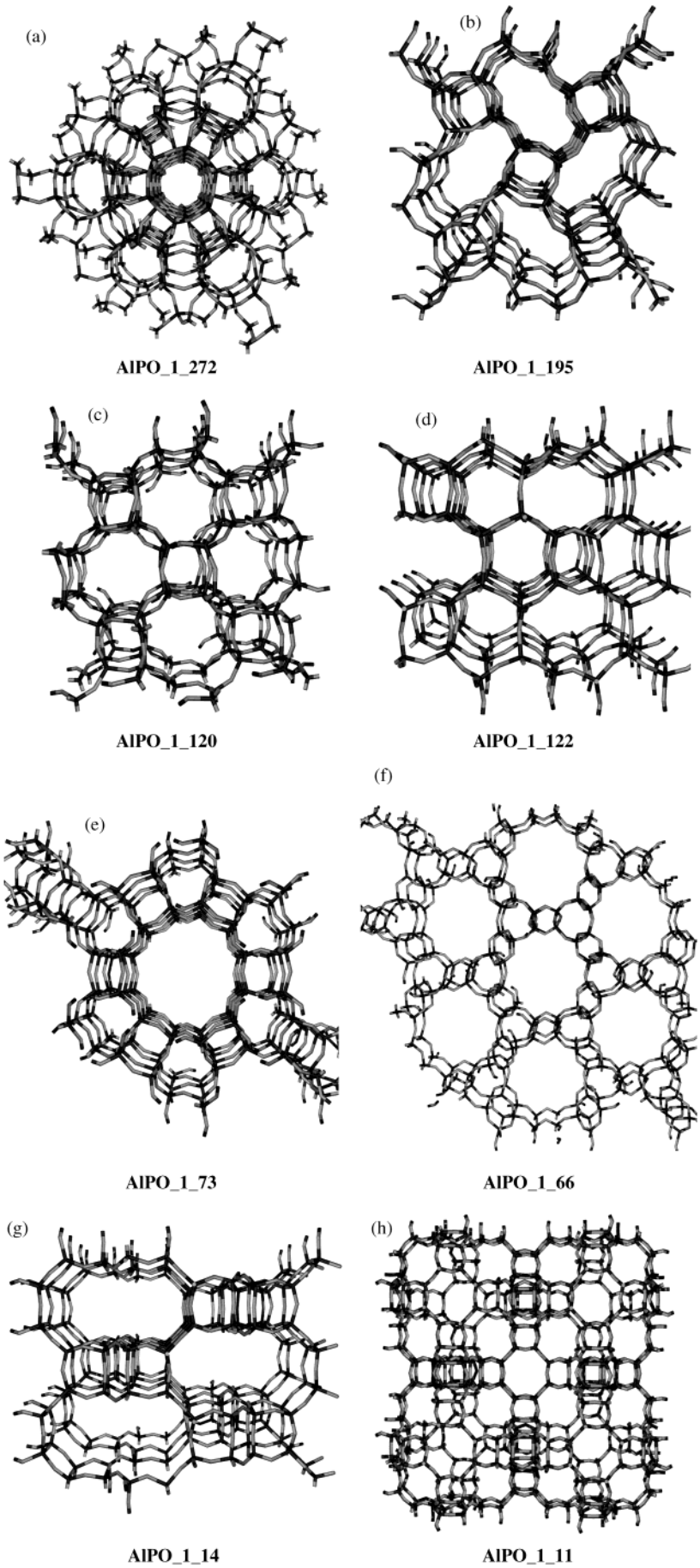

Figure 10. Eight chemically feasible hyp-AlPO structures: (a) AlPO_1_272, (b) AlPO_1_195, (c) AlPO_1_120, (d) AlPO_1_122, (e) AlPO_1_73, (f) AlPO_1_66, (g) AlPO_1_114, and (h) AlPO_1_11.

TABLE 4: Number of T Atoms, Relative Energies, Molar Volumes, Framework Densities, Densities, Cell Parameter, Space Groups, Accessible Volumes, and Total Surface Areas for Eight Selected Hypothetical AlPO (upper part) and Their Isostructural Silica Polymorphs (lower part)[a]

code	T-atoms [kJ/mol]	ΔE_{latt}	V_{mol} [Å^3/mol]	FD [T-sites/ 1000 Å^3]	r [g/cm^3]	a [Å]	*b* [Å]	c [Å]	α [°]	*β* [°]	*γ* [°]	space group	V_{access}/T-site [Å^3]	*S*/T-site [Å^2]
AlPO_1_272	24	2.60	26.08	23.09	2.34	10.13	10.13	10.13	90.00	90.00	90.00	220	0.15	0.04
AlPO_1_195	16	4.40	29.36	20.51	2.08	9.56	9.71	8.40	89.97	89.95	89.99	1	2.47	3.80
AlPO_1_120	16	4.73	32.05	18.79	1.90	9.73	9.92	8.83	90.00	90.00	90.00	60	5.60	9.28
AlPO_1_122	32	4.75	32.43	18.57	1.88	9.15	9.15	20.58	90.02	89.98	90.00	1	6.35	11.13
AlPO_1_73	24	5.93	36.52	16.49	1.67	13.70	13.70	8.96	90.00	90.00	120.00	165	14.17	11.74
AlPO_1_66	36	17.05	34.87	17.27	1.75	22.10	22.10	4.93	90.00	90.00	120.00	148	14.52	10.57
AlPO_1_14	32	18.53	40.01	15.05	1.52	10.12	10.12	20.77	90.00	90.00	90.00	4	18.46	21.20
AlPO_1_11	96	19.11	54.17	11.12	1.13	20.52	20.52	20.52	90.00	90.00	90.00	222	41.27	20.71
ZEO_1_272	24	8.57	25.38	23.73	2.37	10.04	10.04	10.04	90.00	90.00	90.00	230	0.14	0.02
ZEO_1_195	16	10.34	29.88	20.16	2.01	9.75	9.76	8.34	90.00	90.00	90.00	55	4.39	6.91
ZEO_1_120	16	12.78	32.48	18.54	1.85	9.48	10.24	8.89	90.00	90.00	90.00	63	7.11	12.93
ZEO_1_122	32	11.63	31.48	19.13	1.91	9.06	9.06	20.39	90.00	90.00	90.00	141	5.79	10.17
ZEO_1_73	24	13.12	35.42	17.00	1.70	13.55	13.55	8.88	90.00	90.00	120.00	193	13.52	11.39
ZEO_1_66	36	29.55	28.75	20.94	2.09	21.98	21.98	4.97	90.00	90.00	120.00	166	14.83	11.19
ZEO_1_14	32	28.94	39.04	15.43	1.54	10.03	10.03	20.60	90.00	90.00	90.00	141	17.86	20.68
ZEO_1_11	96	29.61	52.85	11.40	1.14	20.35	20.35	20.35	90.00	90.00	90.00	229	40.10	20.17

[a] Note that the numbering AlPO_*n* refers to structures in our database, and not to the AlPO-*n* convention used to identify known AlPO structures.

lattice energies and the population of the fourth coordination shell. This relation serves as another criterion to decide if a structure is feasible or not. Accompanying calculations on known frameworks, which were treated as idealized AlPO and ZEO, confirmed the almost linear relation between stability and density. In addition to stability, an AlPO or ZEO must contain voids or channels to be of interest as a catalyst or sorbent. The accessible volume and the total surface area had to be calculated for each structure. Excellent correlations between accessible volume and framework density prove the internal consistency of our calculation, as well as correlations between surface area and framework density for both known and hypothetical structures. For hypothetical structures, correlations of both the accessible volume and the total surface are almost linear up to a relative lattice energy of 20 kJ/mol, whereas above that value most structures are too dense to have accessible volume/surface and too compressed to be stable. An attempt to find a linear dependence between average geometries and stability revealed that there is none at all. Less stable AlPOs and ZEOs have longer *r*(T−O) bonds and smaller *r*(T···T) distances, while the α(T−O−T) angles are close to 140°, and in some cases slightly below that value. The bond lengths of more stable structures resemble a tight distribution of values, which is expected from GULP calculations with the force fields used. The amount of distortion of the TO_4 units, as obtained by calculating the difference between the largest and smallest tetrahedral angle, is of more interest. Generally, the less stable a structure, the more distorted is the TO_4 unit. A reason is the ionicity of the AlPO: aluminum exists as Al^{3+} cation surrounded by four PO_4^{3-} anions, and oxygen atoms "belong" to the phosphorus rather than to aluminum. For structures below $\Delta E_{latt} = 20$ kJ/mol, all Δα-(O−T−O) distortions are below 11°.

Calculations for the silica polymorphs would be sufficient as a rough guide to stability for both the hypothetical AlPO and ZEO structures, but chemical differences of AlPOs and ZEOs can be revealed only by calculating both the zeotype families with appropriate force fields.

Acknowledgment. We are grateful to the EPSRC and the Leverhulme Trust for funding.

References and Notes

(1) Wells, A. F. *Three-Dimensional Nets and Polyhedra*; Wiley: New York, 1977.
(2) Smith, J. V. *Chem. Rev.* **1988**, *88*, 149.
(3) Akporiaye, D. E.; Price, G. D. *Zeolites* **1989**, *9*, 23.
(4) Akporiaye, D. E.; Price, G. D. *Zeolites* **1989**, *9*, 321.
(5) Han, S.; Smith, J. V. *Acta Crystallogr. A* **1999**, *55*, 332.
(6) Han, S.; Smith, J. V. *Acta Crystallogr. A* **1999**, *55*, 342.
(7) Treacy, M. M. J.; Randall, K. H.; Rao, S.; Perry, J. A.; Chadi, D. J. *Z. Kristallogr.* **1997**, *212*, 768.
(8) Klinowski, J. *Curr. Opin. Solid State Mater. Sci.* **1998**, *3*, 79.
(9) O'Keeffe, M. *Acta Crystallogr. A* **1992**, *48*, 670.
(10) O'Keeffe, M. *Acta Crystallogr. A* **1995**, *51*, 916.
(11) O'Keeffe, M.; Brese, N. E. *Acta Crystallogr. A* **1992**, *48*, 663.
(12) Delgado Friedrichs, O.; Dress, A. W. M.; Huson, D. H.; Klinowski, J.; Mackay, A. L. *Nature* **1999**, *400*, 644.
(13) Foster, M. D.; Delgado Friedrichs, O.; Bell, R. G.; Almeida Paz, F. A.; Klinowski, J. *Angew. Chem., Int. Ed. Engl.* **2003**, *42*, 3896.
(14) Foster, M. D.; Bell, R. G.; Klinowski, J. *Stud. Surf. Sci. Catal.* **2001**, *135*, 16P13.
(15) Wilson, S. T.; Lok, B. M.; Messina, C. A.; Cannan, T. R.; Flanigen, E. M. *J. Am. Chem. Soc.* **1982**, *104*, 1146.
(16) Richardson, J. W., Jr.; Smith, J. V.; Pluth, J. J. *J. Phys. Chem.* **1989**, *93*, 8212.
(17) Corà, F.; Catlow, C. R. A. *J. Phys. Chem. B* **2001**, *105*, 10278.
(18) Piccione, P. M.; Laberty, C.; Yang, S.; Camblor, M. A.; Navrotsky, A.; Davis, M. E. *J. Phys. Chem. B* **2000**, *104*, 10001.
(19) Baerlocher, C.; Hepp, A.; Meier, W. M. DLS-76. A Program for the Simulation of Crystal Structures by Geometric Refinement.; Institut für Kristallographie und Petrographie, ETH: Zürich, Switzerland, 1977.
(20) Gale, J. D. *J. Chem. Soc., Faraday Trans.* **1997**, *93*, 629.
(21) Sanders, M. J.; Leslie, M.; Catlow, C. R. A. *J. Chem. Soc., Chem. Commun.* **1984**, *19*, 1271.
(22) Gale, J. D.; Henson, N. J. *J. Chem. Soc., Faraday Trans.* **1994**, *90*, 3175.
(23) Baerlocher, C.; Meier, W. M.; Olson, D. H. *Atlas of Zeolite Framework Types*, 5th ed.; Elsevier Science B. V.: Amsterdam, 2001.
(24) Cerius2 v. 4.2; Molecular Simulations Inc.: San Diego, 1999.
(25) Sastre, G.; Gale, J. D. *Micropor. Mesopor. Mater.* **2001**, *43*, 27.
(26) Connolly, M. L. *J. Am. Chem. Soc.* **1985**, *107*, 1118.
(27) Hu, N.; Navrotsky, A.; Chen, C.-Y.; Davies, M. E. *Chem. Mater.* **1995**, *7*, 1816.
(28) Richet, P.; Bottinga, Y.; Denielou, L.; Petitet, J. P.; Tequi, C. *Geochim. Cosmochim. Acta* **1982**, *46*, 2639.
(29) Petrovic, I.; Navrotsky, A.; Davis, M. E.; Zones, S. I. *Chem. Mater.* **1993**, *5*, 1805.
(30) Navrotsky, A.; Petrovic, I.; Hu, Y.; Chen, C.-Y.; Davis, M. E. *Micropor. Mater.* **1995**, *4*, 95.
(31) Henson, N. J.; Cheetham, A. K.; Gale, J. D. *Chem. Mater.* **1996**, *8*, 664.
(32) Henson, N. J.; Cheetham, A. K.; Gale, J. D. *Chem. Mater.* **1994**, *6*, 1647.
(33) Brunner, G. O.; Meier, W. M. *Nature* **1989**, *337*, 146.
(34) Hyde, S. T.; Ninham, B. W.; Blum, Z. *Acta Crystallogr. A* **1993**, *49*, 586.
(35) Moloy, E. C.; Davila, L. P.; Shackelford, J. F.; Navrotsky, A. *Micropor. Mesopor. Mater.* **2002**, *54*, 1.